

# Shortcut to Multipartite Entanglement Generation: A Graph Approach to Boson Subtractions

Seungbeom Chin\*

*International Centre for Theory of Quantum Technologies,  
University of Gdańsk, 80-308, Gdańsk, Poland  
Department of Electrical and Computer Engineering,  
Sungkyunkwan University, Suwon 16419, Korea*

Yong-Su Kim

*Center for Quantum Information, Korea Institute of Science and Technology (KIST), Seoul, 02792, Korea  
Division of Nano & Information Technology, KIST School,  
Korea University of Science and Technology, Seoul 02792, Korea*

Marcin Karczewski†

*International Centre for Theory of Quantum Technologies,  
University of Gdańsk, 80-308, Gdańsk, Poland*

Entanglement is a fundamental concept at the core of quantum information science, both in terms of its theoretical underpinnings and practical applications. A key priority in studying and utilizing entanglement is to find reliable procedures for the generation of entangled states. In this research, we propose a graph-based method for systematically searching for schemes that can produce genuine entanglement in arbitrary  $N$ -partite linear bosonic systems, without postselection. While the entanglement generation without postselection renders more tolerable schemes for quantum tasks, it is in general more challenging to find appropriate circuits for systems with a large number of parties. We present a straightforward strategy to mitigate the limitation through the implementation of our graph technique. Our physical setup is based on the sculpting protocol, which utilizes an  $N$  indeterministic subtractions of single bosons to convert Fock states of evenly distributed bosons into entanglement. We have identified general schemes for qubit  $N$ -partite GHZ and W states. These schemes are significantly more efficient than previous schemes. Furthermore, we have found an  $N$ -partite GHZ state generation scheme for qudits, which was never proposed before to our knowledge because of their complicated structures. These results demonstrate the power of our approach in discovering simple solutions for the generation of intricate entangled states. Our schemes can be directly realizable in many-boson systems. As a proof of concept, we propose a linear optical scheme for the generation of the Bell state by heralding detections. Our method has yet to exhaust its potential, and is expected to serve as a promising tool in generating diverse entanglement.

## I. INTRODUCTION

Entanglement is an essential aspect of quantum information science, investigation of which has resulted in new fundamental understandings about the nature [1]. Practically, entanglement is recognized as a valuable resource in the field of quantum information processing, with potential applications in areas such as cryptography [2, 3] and computing [4, 5].

To study and utilize entanglement, it is a prerequisite to find reliable procedures to construct entangled quantum systems. One of the promising approaches to this task is to exploit the indistinguishability of quantum particles [6]. Various works suggested theoretical and experimental entanglement generation schemes based on the iden-

ticality of particles and postselection. Along these lines, Refs. [7–9] showed that two spatially overlapped indistinguishable particles can carry bipartite entanglement. The quantitative relation of particle indistinguishability and spatial overlap to the bipartite entanglement was rigorously analyzed in Refs. [10–12]. For the case of multipartite entanglement, schemes for GHZ and W states with identical particles have been theoretically suggested [13–22] and experimented [23, 24]. Ref. [22] presented a comprehensive graph-theoretic approach to embrace the schemes to generate the entanglement of identical particles in linear quantum networks (LQNs) with postselection.

On the other hand, considering that the postselected schemes are highly sensitive to particle loss in circuits [25, 26] and the multipartite correlations can be created by the postselection bias [27, 28], there have been several attempts to generate the entanglement of identical particles *without postse-*

\* sbthesy@gmail.com

† marcin.karczewski@ug.edu.pl

*lection*. Specifically, heralded generation of entangled states of photons was studied for bipartite [29–32] and multipartite systems [33–38]. Unlike post-selected schemes, heralded ones allow for sorting out the experimental runs for the target state without directly measuring it. While this property of heralded operations renders more tolerable schemes from photon loss [25], it is usually more challenging to find proper circuits to obtain the heralded entanglement of an arbitrary  $N$ -partite systems than the post-selected ones [37].

In this work, we introduce a systematic method to overcome the difficulty of obtaining heralded entanglement generation schemes for an arbitrary  $N$ -partite system. Our method employs the *sculpting protocol* introduced in Ref. [39], which generates an  $N$ -partite entangled state by applying  $N$  single-boson subtraction operators (which we name the “sculpting operator”) to a  $2N$  boson initial state. By setting the initial state to have the even distribution of the bosons in different  $2N$  states (Fig. 1), the indeterministic sculpting operation generates the  $N$ -partite entanglement. And various sculpting operators result in different entangled states. Since linear bosonic systems with heralding detectors can realize boson subtraction operators [40–43], we can design  $N$ -partite genuine entanglement generation schemes with this theoretical process.

In the sculpting protocol, the difficulty of designing a circuit for an  $N$ -partite entangled state is translated to the difficulty of finding a suitable sculpting operator to “chisel” the state. However, former research on the sculpting protocol [39, 44] provides only proof-of-concept schemes demonstrating the method and lacks any systematic way of linking the features of sculpting operators to the expected final states. Our work shows that *a graph picture of the sculpting protocol provides a straightforward strategy of finding appropriate sculpting operators for entanglement, hence appropriate heralding schemes themselves*. We map multi-boson systems with sculpting operators into bipartite graphs (bigraphs), for which we develop techniques to understand key properties of the entanglement generation process. Our list of correspondence relations between sculpting protocols and graphs is a variation of that given in Ref. [10], which provided a systematic method to analyze and design LQNs for obtaining entanglement with postselection. In this graph picture, we have found a special type of bigraphs, which we name *effective perfect matching (EPM) bigraphs*. These bigraphs are highly useful because they can directly correspond to sculpting operators that generate entanglement.

With our graph-theoretic approach, we present

sculpting operators that generate qubit  $N$ -partite GHZ and W states. The GHZ and W schemes are significantly more efficient than those given in Ref. [39], and contrary to the schemes in Refs. [25, 37], general schemes for arbitrary  $N$ -partite entanglement without postselection. To top it off, by generalizing the bigraph used to obtain qubit GHZ states, we also present a *qudit*  $N$ -partite GHZ state generation scheme. To our knowledge, there has been no scheme to generate such states without postselection due to their complicated structure. Our theoretical schemes can be realized in any many-boson system, e.g., linear optical systems with polarization qubit encoding and heralded detections. These outcomes showcase the effectiveness of our method in finding simple solutions for the generation of intricate entangled states.

Our work is organized as follows: Sec. II reviews the sculpting protocol introduced in Ref. [39]. Sec. III explains our dictionary of mapping the sculpting protocol to bigraphs. We also show that the perfect matchings (PMs) of bigraphs determine the final state after the sculpting operation. Sec. IV gives sculpting operators that generate qubit  $N$ -partite GHZ and W states. Using the qubit GHZ generation graph, Sec. V presents a qudit GHZ state generation scheme. Sec. VI explains how linear optical systems with polarization qubit encoding and heralding detectors can build our sculpting schemes. To showcase our method, we present a simple Bell state generation example. Sec. VII summarizes the significance of our results and discusses possible follow-up researches.

## II. SCULPTING PROTOCOL FOR QUBIT ENTANGLEMENT

In this section, we formalize the sculpting protocol [39] that converts the boson identity into entanglement. While  $N$ -partite entangled state was constructed in Ref. [39] based on  $2N$  modes with the dual-rail qubit encoding, we re-explain it based on  $N$  spatial modes and consider the qubit state as a two-dimensional internal degree of freedom of bosons. This way of expression not only embraces the dual-rail encoding, but also provides a more intuitive description of qubit states in the system.

Since in our setup each boson in  $j$ th spatial mode ( $j \in \{1, 2, \dots, N\}$ ) has a two-dimensional internal degree of freedom  $s \in \{0, 1\}$ , boson creation and annihilation operators are denoted as  $\hat{a}_{j,s}^\dagger$  and  $\hat{a}_{j,s}$  respectively. Then, as an input state, we distribute  $2N$  bosons into  $N$  spatial modes so that each mode has two bosons with orthogonal internal states (0

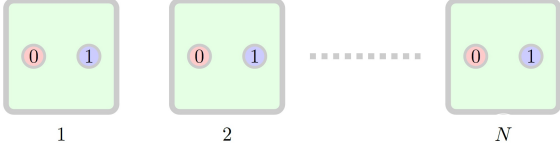


FIG. 1: The initial state  $|Sym_N\rangle$  of  $2N$  bosons in  $N$  spatial modes. Each spatial mode has two bosons, one in the internal state  $|0\rangle$  and the other in  $|1\rangle$ .

and 1, see Fig. 1). Therefore, the initial state is given by

$$\begin{aligned} |Sym_N\rangle &\equiv \hat{a}_{1,0}^\dagger \hat{a}_{1,1}^\dagger \hat{a}_{2,0}^\dagger \hat{a}_{2,1}^\dagger \cdots \hat{a}_{N,0}^\dagger \hat{a}_{N,1}^\dagger |vac\rangle \\ &= \prod_{j=1}^N (\hat{a}_{j,0}^\dagger \hat{a}_{j,1}^\dagger) |vac\rangle. \end{aligned} \quad (1)$$

Following the former works [39, 44], we call it the *maximally symmetric state* of  $2N$  bosons. Rewriting  $|Sym_N\rangle$  in the mode occupation representation as

$$|Sym_N\rangle = |(1, 1), (1, 1), \cdots (1, 1)\rangle \quad (2)$$

and the particle number distribution in the  $2N$  states as a vector, we see that  $|Sym_N\rangle$  is majorized by all the other Fock states of  $2N$  bosons. Several research papers showed that this kind of state is very resourceful in many quantum computation protocols [45–47].

What we need to obtain in the sculpting protocol is a state in which each mode has one boson whose internal state corresponds to the qubit state. For such a final state, we need to annihilate  $N$  single-bosons from the initial state  $|Sym_N\rangle$ . The  $N$  single-boson annihilation operators, which we name the *sculpting operator*, is expressed in the most general form as

$$\begin{aligned} &\prod_{l=1}^N \sum_{j=1}^N (k_{j,0}^{(l)} \hat{a}_{j,0} + k_{j,1}^{(l)} \hat{a}_{j,1}) \\ &\equiv \prod_{l=1}^N \hat{A}^{(l)} \equiv \hat{A}_N. \end{aligned} \quad (3)$$

$(k_{j,s}^{(l)} \in \mathbb{C} \text{ and } \sum_{j,s} |k_{j,s}^{(l)}|^2 = 1)$

We see that the one-boson annihilation operator  $\hat{A}^{(l)}$  can superpose among different spatial modes. Such an operation has been implemented indeterministically in several bosonic experimental setups [40–43].

Applying the sculpting operator  $\hat{A}_N$  to the initial state  $|Sym_N\rangle$ , we obtain the final state,

$$|\Psi\rangle_{fin} = \hat{A}_N |Sym_N\rangle. \quad (4)$$

Note that the correlation of  $|Sym_N\rangle$  from the boson identity and  $\hat{A}_N$  that generates spatial overlap among bosons establish the entanglement property of  $|\Psi\rangle_{fin}$ . Therefore, we can state that *particle identity and spatial overlap are two essential elements for the entanglement generation with sculpting protocol*, as in postselected schemes [9, 12, 24].

There is an essential restriction that we need to impose on a sculpting operator  $\hat{A}_N$ : it must be a superposition of operators that annihilates one particle per spatial mode so that the final total state  $|\Psi\rangle_{fin}$  must consist of states with one particle per mode. Indeed, if  $\hat{A}_N$  can be written as

$$\hat{A}_N = \hat{a}_{k,0} \hat{a}_{k,1} \hat{O}_{(N-2)} + \cdots \quad (k \in \{1, 2, \cdots, N\}) \quad (5)$$

( $\hat{O}_{(N-2)}$  is a multiplication of annihilation operators of order  $N-2$ ), then the final state is given by

$$|\Psi\rangle_{fin} = \hat{O}_{(N-2)} \prod_{j \neq k} \hat{a}_{j,0}^\dagger \hat{a}_{j,1}^\dagger |vac\rangle + \cdots \quad (6)$$

We see that the first term on RHS has at least one mode with two bosons in it. Therefore, we need to adjust  $k_{j,s}^{(l)}$  so that  $\hat{A}_N$  excludes all the terms of the form  $\hat{a}_{k,0} \hat{a}_{k,1} \hat{O}_{(N-2)}$ . We call such a restriction the *no-bunching condition*.

In the dual rail encoding setup [39, 44], the no-bunching condition appears as a seemingly different form. In that setup, repetitive annihilations on the same mode naturally vanish. However, since two modes combine to constitute one subsystem for the case, valid final states are only restricted to those with one boson per two modes. This exactly corresponds to the no-bunching restriction in our setup.

For a later convenience, we rewrite  $\hat{A}^{(l)}$  as

$$\begin{aligned} \hat{A}^{(l)} &= \sum_{j=1}^N (k_{j,0}^{(l)} \hat{a}_{j,0} + k_{j,1}^{(l)} \hat{a}_{j,1}) \\ &\equiv \sum_{j=1}^N \alpha_j^{(l)} \hat{a}_{j, \psi_j^{(l)}} \end{aligned} \quad (7)$$

where  $\alpha_j^{(l)} \in \mathbb{C}$  with  $\sum_j |\alpha_j^{(l)}|^2 = 1$  and  $|\psi_j^{(l)}\rangle$  a normalized qubit state.

All things considered, we summarize the sculpting protocol as follows:

### Sculpting protocol

1. Initial state: We prepare the maximally symmetric state  $|Sym_N\rangle$  of  $2N$  bosons, i.e., each boson has different states (either spatial or internal) with each other as Eq. (32) (see Fig. 1).
2. Operation: We apply the sculpting operator  $\hat{A}_N$  of the form (7) to the initial state  $|Sym_N\rangle$ . *The sculpting process must satisfy the no-bunching condition.*
3. Final state: The final state can be fully separable, partially separable, or genuinely entangled.

Most of the technical difficulty to find  $\hat{A}_N$  for a specific entanglement state comes from Step 2, for it is critical to control the probability amplitudes so that the sculpting operator satisfies the no-bunching restriction. There have been no systematic technique to find suitable  $\hat{A}_N$  that simultaneously satisfies the no-bunching condition and generates non-trivial entanglement state [39]. As we will explain in the following sections, our *graph technique* facilitates a powerful tool to overcome the limitation.

### III. GRAPH PICTURE OF BOSON SYSTEMS WITH SCULPTING OPERATORS

In this section, we present a list of correspondence relations between the fundamental elements of the sculpting protocol and those of graphs. With the mapping, we can replace key physical properties and restrictions on the sculpting operators with those on graphs, which renders a handy guideline to the operator-finding process for genuinely entangled states.

Ref. [22] proposed a list of correspondence relations of linear quantum networks (LQNs) to graphs for providing a systematic method to analyze and design networks for obtaining entanglement without postselection. Since our sculpting protocol also consists of linear transformations of boson annihilation operators, a similar graph mapping dictionary can be imposed to find a suitable  $\hat{A}_N$  that generates genuine entanglement. Indeed, we can map indeterminate annihilation operators into graph elements with a variation of the correspondence relations in Ref. [22], which leads to a practical graph-theoretic method to analyze our system.

The correspondence relations of elements between bosonic systems with sculpting operators and bigraphs can be enumerated as follows:

Boson systems with sculpting operator	Bipartite Graph $G_b = (U \cup V, E)$
Spatial modes	Labelled vertices $\in U$
$\hat{A}^{(l)}$ ( $l \in \{1, 2, \dots, N\}$ )	Unlabelled vertices $\in V$
Spatial distributions of $\hat{A}^{(l)}$	Edges $\in E$
Probability amplitude $\alpha_j^{(l)}$	Edge weight $\alpha_j^{(l)}$
Internal state $\psi_j^{(l)}$	Edge weight $\psi_j^{(l)}$

TABLE I: Correspondence relations of a sculpting operator to a sculpting bigraph

In the above table,  $\alpha_j^{(l)}$  and  $\psi_j^{(l)}$  are defined as in Eq. (7). A brief glossary in graph theory can be found in Ref. [22], Appendix A.

In our graph picture, an annihilation operator  $\hat{A}^{(l)} = \sum_{j=1}^N \alpha_j^{(l)} \hat{a}_{j, \psi_j^{(l)}}$  is mapped to an unlabelled vertex in  $V$  that is connected to labelled vertex  $j$  in  $U$ . Below, unlabelled and labelled vertices are drawn as dots ( $\bullet$ ) and circles ( $\textcircled{j}$ ) respectively. The array of annihilation operators (dots) are on the right hand side of the array of spatial modes (circles). We can consider a more comprehensive mapping including creation operators, which is given in Appendix A. However, Table I suffices to analyze the crucial properties of sculpting operators for generating entanglement.

As a proof of concept, we analyze the simplest  $N = 2$  example with  $\hat{A}_2 = \hat{A}^{(1)} \hat{A}^{(2)}$ . Let us write  $\hat{A}^{(1)}$  and  $\hat{A}^{(2)}$  as

$$\begin{aligned} \hat{A}^{(1)} &= \alpha_1 \hat{a}_{1\psi_1} + \alpha_2 \hat{a}_{2\psi_2}, \\ \hat{A}^{(2)} &= \beta_1 \hat{a}_{1\phi_1} + \beta_2 \hat{a}_{2\phi_2}. \end{aligned} \quad (8)$$

Then  $\hat{A}^{(1)}$  applied to the system is mapped to a bipartite graph (bigraph)

$$\hat{A}^{(1)} = \begin{array}{c} \textcircled{1} \\ \textcircled{2} \end{array} \begin{array}{c} \text{---} (\alpha_1, \psi_1) \text{---} \\ \text{---} (\alpha_2, \psi_2) \text{---} \end{array} \bullet \quad (9)$$

Now, by applying  $\hat{A}^{(2)}$ , the total sculpting operator

$\hat{A}_2$  corresponds to

$$\hat{A}_2 = \hat{A}^{(2)}\hat{A}^{(1)} = \begin{array}{c} \textcircled{1} \xrightarrow{(\alpha_1, \psi_1)} \bullet \\ \textcircled{1} \xrightarrow{(\alpha_2, \psi_2)} \bullet \\ \textcircled{2} \xrightarrow{(\beta_1, \phi_1)} \bullet \\ \textcircled{2} \xrightarrow{(\beta_2, \phi_2)} \bullet \end{array} \quad (10)$$

Note that the physical system is invariant under the exchange of two unlabelled vertices (dots), i.e.,  $\hat{A}_2$  can be also expressed as

$$\hat{A}_2 = \hat{A}^{(1)}\hat{A}^{(2)} = \begin{array}{c} \textcircled{1} \xrightarrow{(\beta_1, \phi_1)} \bullet \\ \textcircled{1} \xrightarrow{(\beta_2, \phi_2)} \bullet \\ \textcircled{2} \xrightarrow{(\alpha_1, \psi_1)} \bullet \\ \textcircled{2} \xrightarrow{(\alpha_2, \psi_2)} \bullet \end{array} \quad (11)$$

This represents nothing but the commutation relation  $[\hat{A}^{(1)}, \hat{A}^{(2)}] = 0$ .

When  $\hat{A}_2$  is expanded as

$$\begin{aligned} \hat{A}_2 &= \hat{A}^{(1)}\hat{A}^{(2)} \\ &= \alpha_1\beta_1\hat{a}_{1\psi_1}\hat{a}_{1\phi_1} + \alpha_1\beta_2\hat{a}_{1\psi_1}\hat{a}_{2\phi_2} \\ &\quad + \alpha_2\beta_1\hat{a}_{2\psi_2}\hat{a}_{1\phi_1} + \alpha_2\beta_2\hat{a}_{2\psi_2}\hat{a}_{2\phi_2}, \end{aligned} \quad (12)$$

each term corresponds to a possible *collective path* (a possible connection of dots to circles in which each dot is uniquely connected to one circle) of the annihilation operators, e.g., the bigraph (10) has four possibilities for two annihilation operators to be applied to the modes. Therefore, the expansion of  $\hat{A}_2$  (12) is expressed with collective paths as

$$\hat{A}_2 = \begin{array}{c} \textcircled{1} \xrightarrow{(\alpha_1, \psi_1)} \bullet \\ \textcircled{1} \xrightarrow{(\beta_1, \phi_1)} \bullet \\ \textcircled{2} \end{array} + \begin{array}{c} \textcircled{1} \xrightarrow{(\alpha_2, \psi_2)} \bullet \\ \textcircled{2} \xrightarrow{(\beta_2, \phi_2)} \bullet \\ \textcircled{2} \end{array}$$

$$+ \begin{array}{c} \textcircled{1} \xrightarrow{(\alpha_1, \psi_1)} \bullet \\ \textcircled{2} \xrightarrow{(\beta_2, \phi_2)} \bullet \end{array} + \begin{array}{c} \textcircled{1} \xrightarrow{(\alpha_2, \psi_2)} \bullet \\ \textcircled{2} \xrightarrow{(\beta_1, \phi_1)} \bullet \end{array}, \quad (13)$$

i.e.,  $\hat{A}_2$  is a superposition of the above four collective paths.

For the sculpting operator  $\hat{A}_2$  to obey the no-bunching condition, we must set the amplitudes so that the first two collective paths in (13) vanish when they are applied to  $|Sym_2\rangle = \hat{a}_{1,0}^\dagger\hat{a}_{1,1}^\dagger\hat{a}_{2,0}^\dagger\hat{a}_{2,1}^\dagger|vac\rangle$ . We can achieve such a sculpting operator by setting

$$\begin{aligned} \alpha_j &= \beta_j = \frac{1}{\sqrt{2}} \quad (j \in \{1, 2\}) \\ |\psi_1\rangle &= |\phi_2\rangle = \frac{1}{\sqrt{2}}(|0\rangle + |1\rangle) \equiv |+\rangle, \\ |\psi_2\rangle &= |\phi_1\rangle = \frac{1}{\sqrt{2}}(|0\rangle - |1\rangle) \equiv |-\rangle. \end{aligned} \quad (14)$$

Then it is direct to check that

$$\begin{aligned} \hat{A}_2|Sym_2\rangle &= \left( \begin{array}{c} \textcircled{1} \xrightarrow{(\frac{1}{\sqrt{2}}, +)} \bullet \\ \textcircled{2} \xrightarrow{(\frac{1}{\sqrt{2}}, +)} \bullet \end{array} + \begin{array}{c} \textcircled{1} \xrightarrow{(\frac{1}{\sqrt{2}}, -)} \bullet \\ \textcircled{2} \xrightarrow{(\frac{1}{\sqrt{2}}, -)} \bullet \end{array} \right) |Sym_2\rangle \\ &= \frac{1}{2}(\hat{a}_{1+}^\dagger\hat{a}_{2+}^\dagger + \hat{a}_{1-}^\dagger\hat{a}_{2-}^\dagger)|vac\rangle, \end{aligned} \quad (15)$$

i.e., by fixing amplitudes as Eq. (14), we obtain a Bell state as the final state.

From the above  $N = 2$  example, we can understand the role of the no-bunching condition in the graph picture. Since the bigraph expression of  $\hat{A}_N$  such as (10) is expanded with a summation of all the possible collective paths of annihilation operators as Eq. (13), we have to control the complex weights of the edges so that any collective path with more than two edges in the same circle does not contribute to the final state. This restriction on bigraphs results in the following property:

**Property 1.** For a specific sculpting operator  $\hat{A}_N$ , the final state  $|\Psi\rangle_{fin} = \hat{A}_N|Sym_N\rangle$  must be fully determined by the addition of the perfect matchings (PMs) of the bigraph corresponding to  $\hat{A}_N$ .

Indeed, we see that the two collective paths in Eq. (15) are the two perfect matchings of the bigraph (10). The above property is useful for understanding given sculpting operators in several aspects, which we explain in Appendix B with a general *sculpting-operator-finding strategy* based on the property. From now on, a bigraph that corresponds to a sculpting operator is called a *sculpting bigraph*.

#### IV. QUBIT ENTANGLEMENT: GHZ AND W STATES

In this section, we present sculpting operators that generate qubit  $N$ -partite GHZ and W states using Property 1. Our operator solutions are more efficient and more feasible to construct in many-boson systems than those given in Ref. [39], especially for the W state case.

To find the sculpting operators for GHZ and W states, we define a specially convenient type of bigraphs, which we dub *effective PM bigraphs*. We restrict our attention to sculpting bigraphs whose edge weights of internal states are only among  $\{|0\rangle, |1\rangle, |+\rangle, |-\rangle\}$  with  $|\pm\rangle \equiv \frac{1}{\sqrt{2}}(|0\rangle \pm |1\rangle)$ .

Among the creation and annihilation operators in the above basis, we can easily see the following identity

$$\forall j \in \{1, 2, \dots, N\},$$

$$\hat{a}_{j,\pm} \hat{a}_{j,0}^\dagger \hat{a}_{j,1}^\dagger |vac\rangle = \pm \hat{a}_{j,\pm}^\dagger |vac\rangle, \quad (16)$$

holds, which directly results in the following identities:

$$\hat{a}_{j,+} \hat{a}_{j,-} \hat{a}_{j,0}^\dagger \hat{a}_{j,1}^\dagger |vac\rangle = 0,$$

$$\hat{a}_{j,0}^n \hat{a}_{j,0}^\dagger \hat{a}_{j,1}^\dagger |vac\rangle = \hat{a}_{j,1}^n \hat{a}_{j,0}^\dagger \hat{a}_{j,1}^\dagger |vac\rangle = 0. \quad (n \geq 2) \quad (17)$$

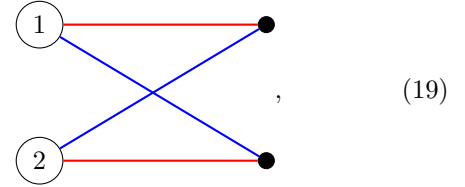
The above identities are translated into our bigraph language as

$$= 0, \quad (18)$$

Here, the internal state edge weights  $\{|0\rangle, |1\rangle, |+\rangle, |-\rangle\}$  are denoted as edge colors  $\{\text{Black, Dotted, Red, Blue}\}$  respectively for the convenience. The amplitude edge weights are

omitted. The translation from Eq. (17) to (18) can be explained more clearly with directed bigraphs (see Appendix A).

Then, we define effective PM bigraphs as *bigraphs whose edges always attach to the circles as one of the above forms*. An example of effective PM bigraphs is the  $N = 2$  bigraph (10) with restrictions (14), i.e.,



because all the edges are attached to the circles as the first form of (18).

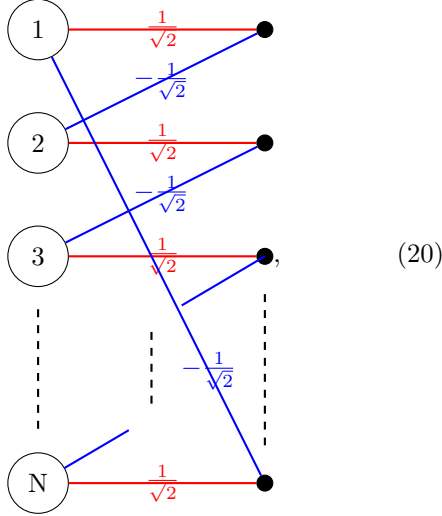
From the identities (18), we can see a crucial property of effective PM bigraphs as follows:

**Property 2.** If a sculpting bigraph is an effective PM bigraph, then the final state is always fully determined by the PMs of the bigraph.

The Combination of Properties 1 and 2 provides a convenient strategy to find sculpting operators that generate a specific entangled state. Since we can express an entangled state with a addition of PMs, *if we can draw an effective PM bigraph which has the same PMs, the bigraph corresponds to a sculpting bigraph that generates the entangled state*. We will show that qubit  $N$ -partite genuinely entangled states, i.e., GHZ and W states, can be generated with such bigraphs.

### A. Qubit GHZ state

The sculpting bigraph that generates the  $N$ -partite GHZ state is given by



where the edge weights represent the probability amplitudes and edge colors Red and Blue represent the internal states  $|+\rangle$  and  $|-\rangle$ . This bigraph was also used in Ref. [22] to obtain the GHZ state in LQNs (see bigraph (30) of Ref. [22]).

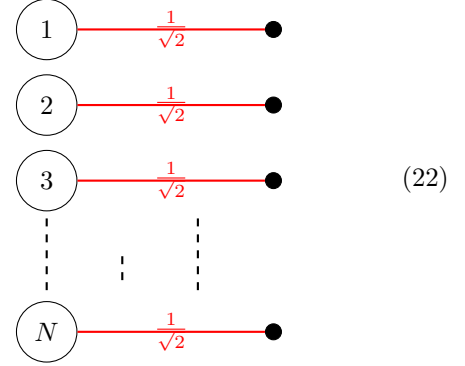
The sculpting operator  $\hat{A}_N$  corresponding to (20) is

$$\begin{aligned} \hat{A}_N &= \frac{1}{\sqrt{2^N}} (\hat{a}_{1,+} - \hat{a}_{2,-}) (\hat{a}_{2,+} - \hat{a}_{3,-}) \cdots \\ &\quad \times (\hat{a}_{N-1,+} \hat{a}_{N,-}) (\hat{a}_{N,+} - \hat{a}_{1,-}) \\ &= \frac{1}{\sqrt{2^N}} \prod_{j=1}^N (\hat{a}_{j,+} - \hat{a}_{j \oplus_N 1,-}), \end{aligned} \quad (21)$$

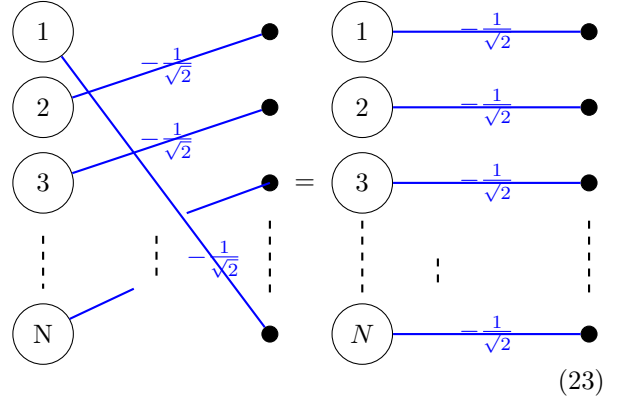
where  $\oplus_N$  in the last line is defined as the addition mod  $N$ .

It is simple to verify that the bigraph (20) corresponds to a sculpting operator that generates the GHZ state. First, the edges of (20) attach to circles as the first of the three graphs in (18). Therefore we see that only the PMs contribute to the final state.

Second, the bigraph has two PMs



and



(the above equality holds since the dots are identical), which constructs the GHZ state.

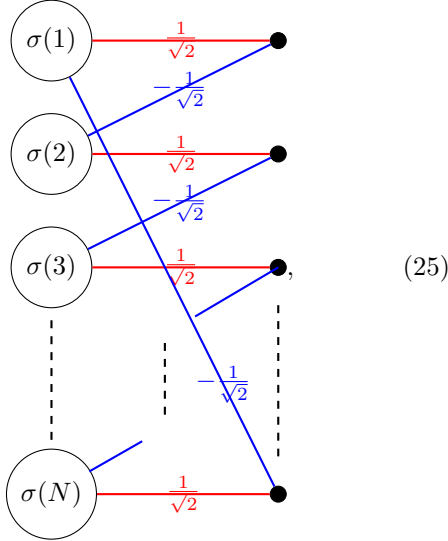
In the operator form, with the identity (16), we see that the final state is explicitly given by

$$\begin{aligned} \hat{A}_N |Sym_N\rangle &= \frac{1}{\sqrt{2^N}} \left( \prod_{j=1}^N \hat{a}_{j,+} + \prod_{j=1}^N \hat{a}_{j,-} \right) |Sym_N\rangle \\ &= \frac{1}{\sqrt{2^N}} \left( \prod_{j=1}^N \hat{a}_{j,+}^\dagger + \prod_{j=1}^N \hat{a}_{j,-}^\dagger \right) |vac\rangle \\ &= \frac{1}{\sqrt{2^{N-1}}} |GHZ_{N,2}\rangle. \end{aligned} \quad (24)$$

From the normalization factor, we directly see that the success probability becomes  $1/2^{N-1}$ .

Note that we can find other sculpting bigraphs for the GHZ state based on (20). While the GHZ state is invariant under the permutation of spatial modes, the bigraph (20) is not. Therefore, any bigraph with the permuted vertex labels of (20) also generates the

GHZ state, i.e.,



under a permutation  $\sigma \in S_N$ . Since the GHZ state is also invariant under the qubit state flip, the exchange of blue and red edges also gives the GHZ state. However, such graph transformations are already included in the above permutation.

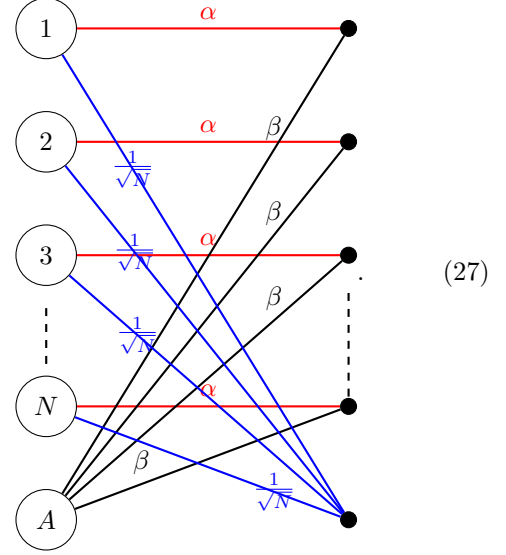
It is worth comparing our GHZ solution (21) with the solution given in Ref. [39],

$$\hat{A}_N = \frac{1}{\sqrt{2^N}} \prod_{l=1}^N \left( \sum_{j=1}^N \hat{a}_{j,0} + \sum_{j=1}^N e^{\frac{2\pi i}{N}(j-l)} \hat{a}_{j,1} \right). \quad (26)$$

Most importantly, the consecutive subtractions in (26) do not remove particles from orthogonal modes. Hence they are very challenging to realize with experimental setups. In contrast, the procedure (21) is based on orthogonal modes, so that a single unitary change of basis is sufficient to prepare all the modes from which a single particle is to be removed. On top of that, each mode in (26) is a weighted superposition of all the initial ones. Understanding the operator from the graph picture, (26) corresponds to a bigraph with  $N^N$  edges. On the other hand, (20) corresponds to a bigraph with only  $2^N$  edges. Therefore, the scheme described by (20) is more effective in the sense that each annihilation operator used there is constructed by superposing just two modes with internal state basis changes.

## B. Qubit W state

A sculpting bigraph for  $N$ -partite W state can be conceived with one ancillary mode as



Edge color Red, Blue, and Black respectively represent the internal state  $|+\rangle$ ,  $|-\rangle$  and  $|0\rangle$ , and  $|\alpha|^2 + |\beta|^2 = 1$ . Circle  $A$  denotes the ancillary mode. Note that this bigraph shares the same permutation symmetry as the W state, i.e., invariance under the permutation of spatial modes.

The sculpting operator corresponding to (27) is given by

$$\begin{aligned} \hat{A}_{N+A} &= (\alpha \hat{a}_{1+} + \beta \hat{a}_{A0}) (\alpha \hat{a}_{2+} + \beta \hat{a}_{A0}) \cdots (\alpha \hat{a}_{N+} + \beta \hat{a}_{A0}) \\ &\quad \times \frac{1}{\sqrt{N}} (\hat{a}_{1-} + \hat{a}_{2-} + \cdots + \hat{a}_{N-}) \\ &= \frac{1}{\sqrt{N}} \left( \prod_{j=1}^N (\alpha \hat{a}_{j+} + \beta \hat{a}_{A0}) \right) \sum_{k=1}^N \hat{a}_{k-}. \end{aligned} \quad (28)$$

The initial state is prepared in a slightly varied way as

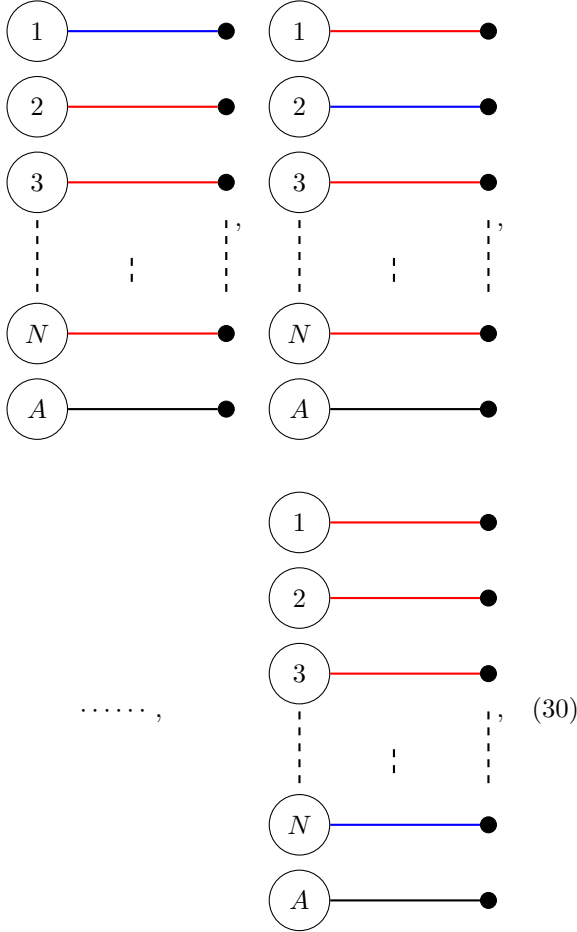
$$|Sym_{N+A}\rangle \equiv \left( \prod_{m=1}^N \hat{a}_{m0}^\dagger \hat{a}_{m1}^\dagger \right) \hat{a}_{A0}^\dagger |vac\rangle, \quad (29)$$

one ancillary boson at the ancillary mode.

It is as manifest as for the GHZ state case to see the above sculpting bigraph (27) generates W state. First, the bigraph is an effective bigraph since edges attach to circles as the first and second graphs in



(18). Second, the above bigraph has  $N$  PMs



which correspond to the W state with an ancillary system.

In the operator form, with the first identity of Eq. (16) again, we have

$$\begin{aligned}
& \hat{A}_{N+A} |Sym_{N+A}\rangle \\
&= \frac{\alpha^{N-1}\beta}{\sqrt{N}} (\hat{a}_{1-}\hat{a}_{2+}\cdots\hat{a}_{N+} + \hat{a}_{1+}\hat{a}_{2-}\cdots\hat{a}_{N+} \\
&\quad + \cdots + \hat{a}_{1+}\hat{a}_{2+}\cdots\hat{a}_{N-}) \\
&\quad \times \hat{a}_{A0}\hat{a}_{A0}^\dagger \prod_{m=1}^N \hat{a}_{m0}^\dagger \hat{a}_{m1}^\dagger |vac\rangle \\
&= \frac{\alpha^{N-1}\beta}{\sqrt{N}} (\hat{a}_{1-}^\dagger \hat{a}_{2+}^\dagger \cdots \hat{a}_{N+}^\dagger + \hat{a}_{1+}^\dagger \hat{a}_{2-}^\dagger \cdots \hat{a}_{N+}^\dagger \\
&\quad + \cdots + \hat{a}_{1+}^\dagger \hat{a}_{2+}^\dagger \cdots \hat{a}_{N-}^\dagger) |vac\rangle \\
&= \alpha^{N-1}\beta |W_N\rangle. \tag{31}
\end{aligned}$$

The success probability is  $|\alpha^{N-1}\beta|^2$ , whose maximal value becomes  $\frac{(N-1)^{N-1}}{\sqrt{N}}$  when  $|\alpha| = \sqrt{\frac{N-1}{N}}$  and  $|\beta| = \frac{1}{\sqrt{N}}$ .

We can also check that this bigraph can be used to generate W state in LQNs with postselection. Indeed, by drawing a bigraph that corresponds to the schemes suggested in Ref. [16, 17], we obtain the same form of bigraph with (30).

Comparing with the W state generation scheme suggested in Ref. [39], we can easily see that our current scheme have accomplished an outstanding improvement. The scheme in Ref. [39] starts from  $4N$  bosons in  $2N$  modes and goes through two steps of sculpting to generate the final  $N$ -partite W state. On the other hand, using the graph mapping technique, we have obtained a much more efficient  $N$ -partite W-state generation scheme just with  $2N + 1$  bosons in  $N + 1$  modes and one simple step of sculpting.

## V. QUDIT ENTANGLEMENT: GHZ STATE

Our graph picture also provides a useful insight to find sculpting operators for the general *qudit* systems. We will present in this section a sculpting bigraph for the qudit  $N$ -partite GHZ state, which has a generalized form of the qubit GHZ bigraph (35).

The qudit state is represented by a  $d$ -dimensional internal degree of freedom  $s$  ( $\in \{0, 1, \dots, d\}$ ) of bosons. To construct  $N$  partite qudit genuinely entangled states, we initially distribute  $dN$  bosons into  $N$  modes so that exactly  $d$  bosons with mutually orthogonal internal states belong to a spatial mode (see Fig. 2). Hence, the initial state is given by

$$|Sym_{N,d}\rangle \equiv \prod_{j=1}^N (\hat{a}_{j,0}\hat{a}_{j,1}\cdots\hat{a}_{j,d})|vac\rangle. \tag{32}$$

Here  $|Sym_{N,d}\rangle$  denotes the  $N$  mode maximally symmetric state with a  $d$ -dimensional internal degree of freedom.

The sculpting operator

$$\hat{A}_N = \prod_{l=1}^{(d-1)N} \hat{A}^{(l)} \tag{33}$$

must be set to extract  $(d - 1)$  bosons per mode so that one boson per mode in the final state determines the qudit state of each subsystem. All in all, the sculpting protocol is modified for qudits as follows:

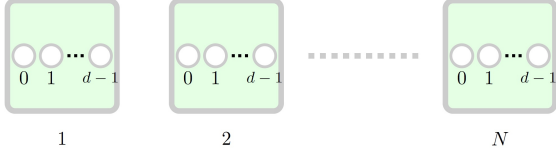


FIG. 2: The initial state  $|Sym_{N,d}\rangle$  of  $dN$  bosons in  $N$  spatial modes. Each mode has  $d$  bosons, which have mutually orthogonal internal states  $|0\rangle, |1\rangle, \dots, |d-1\rangle$ .

### Sculpting protocol of qudits

1. Initial state: We prepare the maximally symmetric state  $|Sym_{N,d}\rangle$  of  $dN$  bosons, i.e., each boson has different states (either spatial or internal) with each other as Eq. (32). See Fig. 2.
2. Operation: We apply the sculpting operator  $\hat{A}_N$  to the initial state  $|Sym_{N,d}\rangle$ . The sculpting operator must be set to extract  $(d-1)$  bosons per mode.
3. Final state: The final state can be fully separable, partially separable, or genuinely entangled.

Now we provide a sculpting operator that generates the  $N$ -partite GHZ state of  $d$ -level systems, denoted as  $|GHZ_{N,d}\rangle$ , by generalizing the qubit GHZ sculpting operator in Sec. IV A.

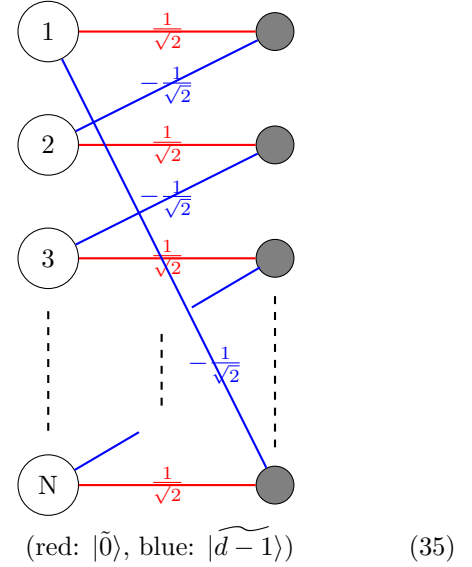
First, by generalizing the  $d = 2$  basis set  $\{|+\rangle, |-\rangle\}$  for the internal states of the sculpting operators, we choose the arbitrary  $d$ -dimensional basis set  $\{|\tilde{k}\rangle\}_{k=0}^{d-1}$  where

$$|\tilde{k}\rangle = \frac{1}{\sqrt{d}} \left( |0\rangle + \omega^k |1\rangle + \omega^{2k} |2\rangle + \dots + \omega^{(d-1)k} |d-1\rangle \right) \quad (34)$$

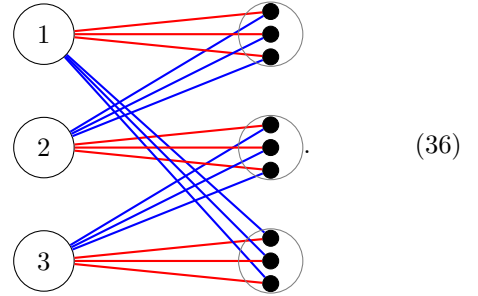
( $\omega = e^{i\frac{2\pi k}{d}}$ ) for the internal states of the sculpting operators.

Second, we use an overlap of  $(d-1)$  copies of the graph (20) for the sculpting bigraph, i.e., the following bigraph corresponds to the sculpting operator

for the GHZ state:



where a gray circle represents a group of  $(d-1)$  identical vertices that have the same edges. For example, when  $N = 3$  and  $d = 4$ , the above graph is explicitly drawn as



The sculpting operator that corresponds to the bigraph (35) is given by

$$\begin{aligned} \hat{A}_{N,d} &= \left( \frac{1}{\sqrt{2}} \right)^{(d-1)N} (\hat{a}_{1,\tilde{0}} - \hat{a}_{2,\widetilde{d-1}})^{d-1} (\hat{a}_{2,\tilde{0}} - \hat{a}_{3,\widetilde{d-1}})^{d-1} \\ &\quad \times (\hat{a}_{3,\tilde{0}} - \hat{a}_{4,\widetilde{d-1}})^{d-1} \dots \times (\hat{a}_{N,\tilde{0}} - \hat{a}_{1,\widetilde{d-1}})^{d-1}. \end{aligned} \quad (37)$$

We verify that the above operator constructs the qudit  $N$ -partite GHZ state in Appendix C. To catch the sense of how the graph (35) works, we explicitly explain the qutrit case ( $d = 3$ ) here.

### A. Qutrit GHZ state

For a qutrit system, the basis set (34) is given by

$$\begin{aligned} \{|\tilde{0}\rangle &= \frac{1}{\sqrt{3}}(|0\rangle + |1\rangle + |2\rangle), \\ |\tilde{1}\rangle &= \frac{1}{\sqrt{3}}(|0\rangle + e^{i\frac{2\pi}{3}}|1\rangle + e^{i\frac{4\pi}{3}}|2\rangle), \\ |\tilde{2}\rangle &= \frac{1}{\sqrt{3}}(|0\rangle + e^{i\frac{4\pi}{3}}|1\rangle + e^{i\frac{2\pi}{3}}|2\rangle)\}. \end{aligned} \quad (38)$$

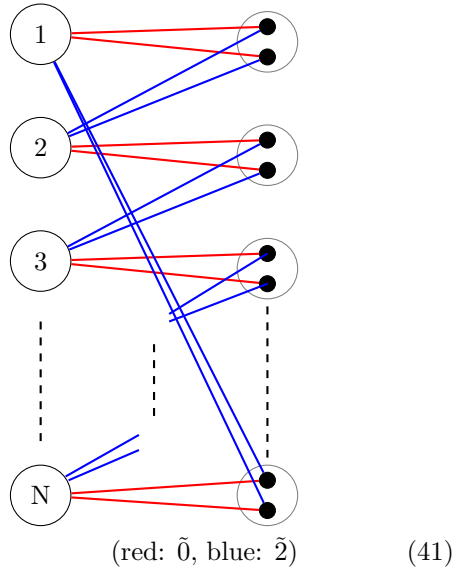
Then, we directly check that the following identities hold:

$$\begin{aligned} (\hat{a}_{j,\tilde{0}})^2 \hat{a}_{j,0}^\dagger \hat{a}_{j,1}^\dagger \hat{a}_{j,2}^\dagger &= \frac{2}{\sqrt{3}} \hat{a}_{j,\tilde{0}}^\dagger, \\ \hat{a}_{j,\tilde{0}} \hat{a}_{j,\tilde{2}} \hat{a}_{j,0}^\dagger \hat{a}_{j,1}^\dagger \hat{a}_{j,2}^\dagger &= -\frac{1}{\sqrt{3}} \hat{a}_{j,\tilde{1}}^\dagger, \\ (\hat{a}_{j,\tilde{2}})^2 \hat{a}_{j,0}^\dagger \hat{a}_{j,1}^\dagger \hat{a}_{j,2}^\dagger &= \frac{2}{\sqrt{3}} \hat{a}_{j,\tilde{2}}^\dagger. \end{aligned} \quad (39)$$

(note that the above identities are also obtained from Eq. (C1) with  $d = 3$ ). From the second identity of the above, we can see that

$$(\hat{a}_{j,\tilde{0}})^2 \hat{a}_{j,\tilde{2}} \hat{a}_{j,0}^\dagger \hat{a}_{j,1}^\dagger \hat{a}_{j,2}^\dagger = \hat{a}_{j,\tilde{0}} (\hat{a}_{j,\tilde{2}})^2 \hat{a}_{j,0}^\dagger \hat{a}_{j,1}^\dagger \hat{a}_{j,2}^\dagger = 0 \quad (40)$$

also holds. The graph (35) for  $d = 3$  is now drawn as



and the corresponding sculpting operator becomes

$$\begin{aligned} \hat{A}_{N,3} &= \left(\frac{1}{\sqrt{2}}\right)^{2N} (\hat{a}_{1,\tilde{0}} - \hat{a}_{2,\tilde{2}})^2 (\hat{a}_{2,\tilde{0}} - \hat{a}_{3,\tilde{2}})^2 \\ &\quad \times (\hat{a}_{3,\tilde{0}} - \hat{a}_{4,\tilde{2}})^2 \times \cdots \times (\hat{a}_{N,\tilde{0}} - \hat{a}_{1,\tilde{2}})^2. \end{aligned} \quad (42)$$

Then, the final state is given by

$$\begin{aligned} \hat{A}_{N,3} |\text{Sym}_{N,3}\rangle &= \left(\frac{1}{\sqrt{2}}\right)^{2N} \left( \prod_{r=1}^N (\hat{a}_{r,\tilde{0}})^2 + \prod_{s=1}^N (-2\hat{a}_{s\tilde{0}} \hat{a}_{s\tilde{2}}) + \prod_{t=1}^N (\hat{a}_{t,\tilde{2}})^2 \right) \\ &\quad \times \prod_{p=1}^N \hat{a}_{p,0}^\dagger \hat{a}_{p,1}^\dagger \hat{a}_{p,2}^\dagger |\text{vac}\rangle \\ &= \left(\frac{1}{\sqrt{3}}\right)^N \left( \prod_{r=1}^N \hat{a}_{r,\tilde{0}}^\dagger + \prod_{s=1}^N \hat{a}_{s\tilde{1}}^\dagger + \prod_{t=1}^N \hat{a}_{t,\tilde{2}}^\dagger \right) |\text{vac}\rangle \\ &= \left(\frac{1}{\sqrt{3}}\right)^{N-1} |\text{GHZ}_{N,3}\rangle. \end{aligned} \quad (43)$$

The second line is obtained by Eq. (40) and the third by Eq. (39). The success probability is  $1/3^{N-1}$ .

*Remark.* — To the best of our knowledge, there has been no scheme proposed to generate an  $N$ -partite GHZ state for an arbitrary  $d$  dimensions. For example, Ref. [48] just proposed heralded schemes for the 4-dimensional four photon GHZ state and 3-dimensional Bell state. Moreover, we can generalize the concept of EPM bigraphs for qudit cases, which we believe guarantees several schemes for various qudit entangled states.

## VI. HERALDED SCHEME OF SCULPTING PROTOCOLS IN LINEAR OPTICS: BELL STATE EXAMPLE

We can realize the sculpting protocol in various multi-boson systems. There are general schemes in optics [40–43] and trapped-ions [49] to establish indeterministic annihilation operators of bosons. Based on such methods, Ref. [39] proposed an optical scheme for constructing sculpting operators. More recently, Ref. [44] suggested an experimental scheme with arithmetic annihilations of trapped ions to generate the GHZ state with the sculpting operator (26) in Ref. [39]. Both works are based on the dual-rail qubit encoding.

Here, we propose an alternative optical scheme to execute the sculpting protocol with polarization qubit encoding and heralding detections. In this setup, we set the internal boson states  $\{|0\rangle, |1\rangle\}$  as the polarization of photons  $\{|D\rangle, |A\rangle\}$ , with

$$\begin{aligned} |+\rangle &\rightarrow |H\rangle = \frac{1}{\sqrt{2}}(|D\rangle + |A\rangle), \\ |-\rangle &\rightarrow |V\rangle = \frac{1}{\sqrt{2}}(|D\rangle - |A\rangle). \end{aligned} \quad (44)$$

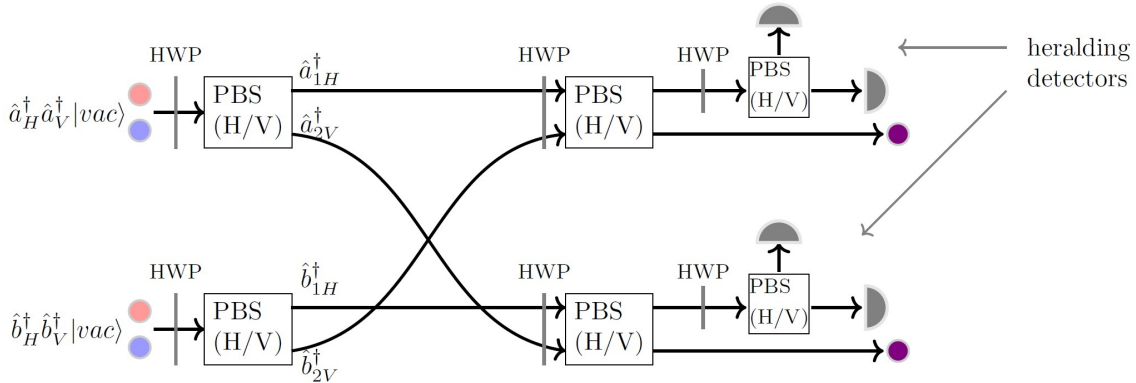


FIG. 3: Linear optical circuit for generating the Bell state. Annihilation operators are realized by sending photons indeterministically to heralding detectors. The two heralding detectors sort out only the cases when each detector observes one photon.

And the initial state is given by

$$|Sym_N\rangle = \prod_{j=1}^N \hat{a}_{j,D}^\dagger \hat{a}_{j,A}^\dagger. \quad (45)$$

As the simplest nontrivial example, we present a linear optical circuit to generate the Bell state. The optical elements used in the circuit can be applied to more general multipartite entangled states. Our circuit design is based on the sculpting bigraph (10) by fixing edge weights as in Eq. (14). Fig. 3 shows our experimental scheme. The initial state is prepared as

$$\hat{a}_H^\dagger \hat{a}_V^\dagger \hat{b}_H^\dagger \hat{b}_V^\dagger |vac\rangle, \quad (46)$$

where  $\hat{a}^\dagger$  and  $\hat{b}^\dagger$  are creation operators for two spatial modes. To take the sculpting operator

$$\hat{A}_2 = \frac{1}{2}(\hat{a}_H + \hat{b}_V)(\hat{a}_H + \hat{b}_V), \quad (47)$$

we rotate the initial state into the  $D/A$  direction with half-wave plates (HWP) and send them through polarizing beam splitters (PBS). We place PBSs so that the photon path follows the sculpting bigraph (10). By selecting only the cases when each detector detects a single photon, we generate Bell states as expected. Appendix D explains the photon state evolution in detail. The optical circuit is highly feasible as it employs only HWPs and PBSs to construct photon annihilation operators.

To realize sculpting out photons of internal states  $\{|+\rangle, |-\rangle\}$  (see sculpting bigraphs (20) and (27)), we rotate the polarization of photons to  $90^\circ$  and send photons indeterministically to heralding detectors. We attach a heralding detector per mode to sort out the cases when the extraction fits in with the sculpting operator.

## VII. DISCUSSIONS

We have proposed a systematic approach for finding entanglement generation schemes based on linear bosonic systems with heralding. It proceeds in two steps: first, we find a theoretical sculpting operator that generates an entangled state. Second, we construct a concrete experimental circuit for such a sculpting operator. In the process of finding sculpting operators, we have exploited graph techniques by imposing the correspondence relations of bosonic systems to bigraphs. We have shown that the graph picture of bosonic systems facilitates a powerful tool to find proper sculpting operators. The theoretical schemes can be realized in any many-boson systems. As the simplest example, we have presented a Bell state circuit in linear optics with polarized photons, which can be generalized to other schemes that we have proposed.

As explained, our graph approach presents a straightforward strategy for finding multipartite entangled states without postselection. Hence, it suggests several interesting research directions. First, as a next step towards the realization of our theoretic-

cal schemes, it is essential to design experimental circuits of qubit GHZ and W states with polarized photons based on the optical elements given in Sec. VI. While most of former works on generating genuine entangled states remain in tripartite cases [25, 37], optical circuits based on our theoretical scheme will be generalized to an arbitrary  $N$ -partite case. We can also conceive a general transformation rule from a given sculpting bigraph to a linear optical network to generate entanglement (SC, MK, and YSK, in preparation). For the case of qudit GHZ state, one can encode qudit states with the orbital angular momentum (OAM) of photons [50]. Second, our formalism and strategy can be extended to encompass more complex qudit systems. We have introduced EPM bigraphs for finding qubit solutions, which can be generalized to qudit cases. Third, in the same context with the above, our sculpting protocol can identify other interesting qudit multipartite entangled states. Since our graph approach provides a handy guideline to coming up with useful sculpting operators, we expect that it could be used to find heralded schemes for, e.g., graph states [51],  $N$ -particle  $N$ -level singlet states [52], cyclically symmetric states [53], and other less symmetric genuinely entangled states.

## COMPETING INTERESTS

All authors declare no competing interests.

## AUTHOR CONTRIBUTIONS

SC and MK organized the project. SC was responsible for the methodology, solutions, and the manuscript as the first author and one of the co-corresponding authors. MK contributed to the theory and writing as one of the co-corresponding authors. YSK worked on the optical circuit of the Bell state as a co-author.

## ACKNOWLEDGEMENTS

SC is grateful to Prof. Ana Belen Sainz and Prof. Jung-Hoon Chun for their support on this research. This research is funded by National Research Foundation of Korea (NRF, 2019R1I1A1A01059964, 2021M3H3A103657313, and 2022M3K4A1094774), Korea Institute of Science and Technology (2E31021), and Foundation for Polish Science (IRAP project, ICTQT, contract no.2018/MAB/5, co-financed by EU within Smart Growth Operational Programme).

### Appendix A: Directed bigraph mapping of many-boson systems with creation and annihilation operators

In Section III of the main content, we have presented a list of correspondence relations between sculpting operators and bigraphs. Even if the list suffices to explain our sculpting protocol, we can propose a comprehensive *directed* graph mapping of many-boson systems including both creation and annihilation operators.

In this directed graph mapping, both creation and annihilation operators correspond to unlabelled vertices. They are distinguished by the direction of edges attached to them as the following table. In other words, *creation (annihilation) operators are denoted as unlabelled vertices whose edges go to (come from) circles*. The other correspondence relations are not changed from Table I of the main content.

The directed graph mapping is useful to describe the thorough process of sculpting protocol. The initial state (32) is drawn in a directed graph as

$$|Sym_N\rangle = \prod_{j=1}^N (\hat{a}_{j,0}^\dagger \hat{a}_{j,1}^\dagger) |vac\rangle = \begin{array}{c} \bullet \longrightarrow \textcircled{1} \\ \bullet \cdots \longrightarrow \textcircled{1} \\ \bullet \longrightarrow \textcircled{2} \\ \bullet \cdots \longrightarrow \textcircled{2} \\ \vdots \\ \bullet \longrightarrow \textcircled{N} \\ \bullet \cdots \longrightarrow \textcircled{N} \end{array} \quad (\text{A1})$$

For example, the  $N = 2$  Bell state generating scheme with a sculpting bigraph (19) is expressed as the following directed bigraph

$$|\Psi\rangle_{fin} = \hat{A}_2 |Sym_2\rangle = (\hat{A}^{(1)} \hat{A}^{(2)}) \hat{a}_{1,0}^\dagger \hat{a}_{1,1}^\dagger \hat{a}_{2,1}^\dagger \hat{a}_{2,1}^\dagger |vac\rangle = \begin{array}{c} \bullet \longrightarrow \textcircled{1} \xrightarrow{\text{red}} \bullet \\ \bullet \cdots \longrightarrow \textcircled{1} \xrightarrow{\text{blue}} \bullet \\ \bullet \longrightarrow \textcircled{2} \xrightarrow{\text{blue}} \bullet \\ \bullet \cdots \longrightarrow \textcircled{2} \xrightarrow{\text{red}} \bullet \end{array} \quad (\text{A2})$$

The directed bigraphs present a clear diagrammatic understanding of the identities (16) and (17), which are translated into directed bigraphs respectively as

$$\begin{array}{c} \bullet \cdots \longrightarrow \textcircled{j} \\ \bullet \longrightarrow \textcircled{j} \end{array} \xrightarrow{\text{red}} \bullet = \bullet \xrightarrow{\text{red}} \textcircled{j}, \quad \begin{array}{c} \bullet \longrightarrow \textcircled{j} \\ \bullet \cdots \longrightarrow \textcircled{j} \end{array} \xrightarrow{\text{blue}} \bullet = - \bullet \xrightarrow{\text{blue}} \textcircled{j} \quad (\text{A3})$$

and

$$\begin{array}{c} \bullet \longrightarrow \textcircled{j} \xrightarrow{\text{red}} \bullet \\ \bullet \cdots \longrightarrow \textcircled{j} \xrightarrow{\text{blue}} \bullet \end{array} = 0, \quad \begin{array}{c} \bullet \longrightarrow \textcircled{j} \xrightarrow{\text{red}} \bullet \\ \bullet \cdots \longrightarrow \textcircled{j} \xrightarrow{\text{red}} \bullet \end{array} = 0, \quad \begin{array}{c} \bullet \longrightarrow \textcircled{j} \xrightarrow{\text{red}} \bullet \\ \bullet \cdots \longrightarrow \textcircled{j} \xrightarrow{\text{red}} \bullet \\ \bullet \longrightarrow \textcircled{j} \xrightarrow{\text{blue}} \bullet \\ \bullet \cdots \longrightarrow \textcircled{j} \xrightarrow{\text{blue}} \bullet \end{array} \xrightarrow{\text{red}} \bullet = \begin{array}{c} \bullet \longrightarrow \textcircled{j} \xrightarrow{\text{red}} \bullet \\ \bullet \cdots \longrightarrow \textcircled{j} \xrightarrow{\text{red}} \bullet \\ \bullet \longrightarrow \textcircled{j} \xrightarrow{\text{blue}} \bullet \\ \bullet \cdots \longrightarrow \textcircled{j} \xrightarrow{\text{blue}} \bullet \end{array} \xrightarrow{\text{blue}} \bullet = 0. \quad (\text{A4})$$

By omitting the left part of circles, the above relations become the bigraph identities (18) of the main content.

## Appendix B: Sculpting-operator-finding strategy

In this section, we briefly explain the advantage of Property 1 that links the final entangled state and perfect matchings (PMs) of sculpting bigraphs. Even if we have found sculpting operators that generates entanglement by combining it with Property 2 in the main content, there are several reasons that Property 1 itself provides useful insight to analyze sculpting operators that do not correspond to effective PM diagrams.

First, for a given bigraph that corresponds to a sculpting operator, we can immediately read the possible final state from the PMs of the bigraph. For the  $N = 2$  example, we can expect from (13) that  $\hat{A}_2$  has the potential to generate the Bell state before fixing the amplitudes.

Second, we can apply all the PM diagram techniques developed in Ref. [22] to our system. Since the final states in both approaches correspond to the summation of PMs in a given bigraph, necessary conditions for a bigraph to carry genuine entanglement in LQNs (see Theorem 1 of Ref. [22]) are also valid to our protocol.

Third, in the same context as the second reason, we can consider bigraphs that generate entanglement in LQNs [22] as strong candidates for sculpting operators that generate entanglement in our protocol.

Based on these advantages, we can build a strategy to find sculpting operator for a genuinely entangled state [54].

### Sculpting-operator-finding strategy

1. Write down all the states that consist of the entangled state that we want to generate. Draw the PMs that correspond to the states.
2. Draw a bigraph that has the above PMs. We choose a bigraph with minimal edges so that it has minimal collective paths.
3. Examine whether we can set the edge weights so that only PMs among the collective paths contribute to the final state.
4. If we can find such an edge weight solution, it corresponds to the sculpting operators that generates the entangled state we expect. If we cannot, we try other bigraph with the same PMs but more edges.

In Step 2, we can use, e.g., a method suggested in Ref. [22], Sec. III.B to find bigraphs for a specific set of PMs. Note that Step 2 provides a significant benefit since reducing edges in bigraphs means reducing the number of possible no-bunching restrictions that we have to consider. Furthermore, a sculpting operator found in that way usually can be constructed more efficiently since a smaller number of edges implies a small amount of resource to create operator superpositions. One can understand the edge number as the coherence number [55] of a quantum state, which is a coherence monotone that quantifies the amount of coherence in a quantum system. Therefore, we can consider in a general sense that a system corresponding to a bigraph with more edges needs more quantum resource.

## Appendix C: Qudit GHZ state

To show that  $\hat{S}_{GHZN,d}|Sym_{N,d}\rangle$  constructs the GHZ state, we use the following identities:

$$\begin{aligned}
 (\hat{a}_0)^l (\hat{a}_{\widetilde{d-1}})^{d-1-l} \prod_{s=0}^{d-1} \hat{a}_s^\dagger &= (-1)^{(d-1-l)} \frac{l!(d-1-l)!}{\sqrt{d}^{d-2}} \hat{a}_{\widetilde{d-1-l}}^\dagger \quad (l \in \{0, 1, \dots, d-1\}), \\
 (\hat{a}_0)^m (\hat{a}_{\widetilde{d-1}})^{d-m} \prod_{s=0}^{d-1} \hat{a}_s^\dagger &= 0 \quad (m \in \{1, \dots, d-1\}).
 \end{aligned} \tag{C1}$$

In the above equations, we can check that the second identity is directly obtained by taking  $\hat{a}_0$  or  $\hat{a}_{\widetilde{d-1}}$  to the first identity.

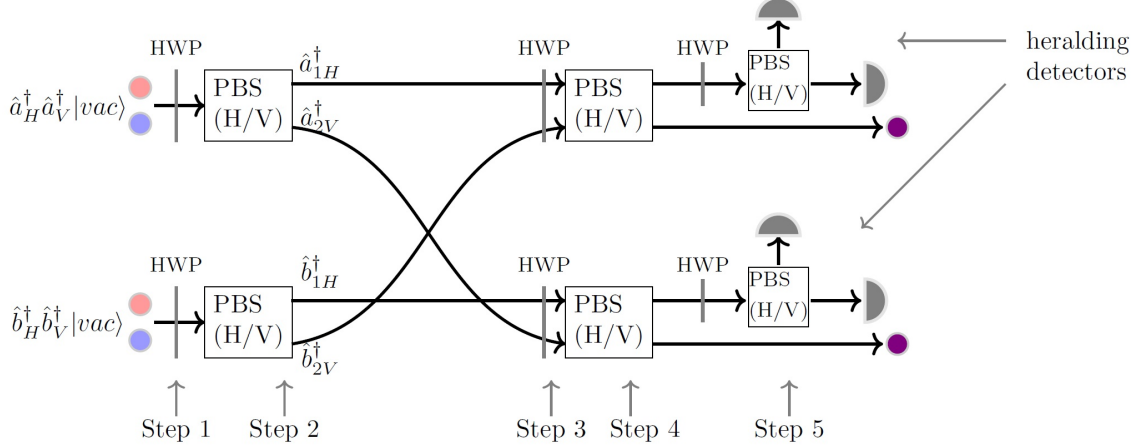


FIG. 4: Linear optical circuit for generating the Bell state by 5 steps

Then the sculpting operator (37) is expanded as

$$\begin{aligned} \hat{S}_{GHZ_d} &= \left(\frac{1}{\sqrt{2}}\right)^{(d-1)N} (\hat{a}_{1,\bar{0}} - \hat{a}_{2,\bar{d-1}})^{d-1} (\hat{a}_{2,\bar{0}} - \hat{a}_{3,\bar{d-1}})^{d-1} \cdots (\hat{a}_{N,\bar{0}} - \hat{a}_{1,\bar{d-1}})^{d-1} \\ &= \left(\frac{1}{\sqrt{2}}\right)^{(d-1)N} \left[ \sum_{l_1=0}^{d-1} \binom{d-1}{l_1} (\hat{a}_{1,\bar{0}})^{l_1} (\hat{a}_{2,\bar{2}})^{d-1-l_1} \right] \cdots \left[ \sum_{l_N=0}^{d-1} \binom{d-1}{l_N} (\hat{a}_{N,\bar{0}})^{l_N} (\hat{a}_{0,\bar{2}})^{d-1-l_N} \right]. \end{aligned} \quad (C2)$$

Then, using identities (C1), we have

$$\begin{aligned} \hat{S}_{GHZ_d} |Sym_d\rangle &= \left(\frac{1}{\sqrt{2}}\right)^{(d-1)N} \sum_l \left[ \binom{d-1}{l} \right]^N (-1)^{N(d-1-l)} \prod_{k=1}^N \left( \hat{a}_{k,\bar{0}}^l \hat{a}_{k,\bar{d-1}}^{d-1-l} \left( \prod_{s=0}^{d-1} \hat{a}_{k,s}^\dagger \right) \right) \\ &= \left( \frac{(d-1)!}{\sqrt{2}^{d-1} \sqrt{d}^{d-2}} \right)^N (|\tilde{0}, \tilde{0}, \dots, \tilde{0}\rangle + \cdots + |\tilde{d-1}, \tilde{d-1}, \dots, \tilde{d-1}\rangle), \end{aligned} \quad (C3)$$

i.e., the qudit GHZ state in the quantum Fourier transformed basis.

#### Appendix D: Bell state generation in optics

In this section, we explain the photon state evolution of our experimental scheme presented in Sec. VI. The state evolution consists of 5 steps as denoted in Fig. 4.

- Step 1

$$\hat{a}_H^\dagger \hat{a}_V^\dagger \hat{b}_H^\dagger \hat{b}_V^\dagger |vac\rangle \rightarrow \hat{a}_D^\dagger \hat{a}_A^\dagger \hat{b}_D^\dagger \hat{b}_A^\dagger |vac\rangle \quad (D1)$$

- Step 2

$$\frac{1}{4} (\hat{a}_{1H}^\dagger + \hat{a}_{2V}^\dagger) (\hat{a}_{1H}^\dagger - \hat{a}_{2V}^\dagger) (\hat{b}_{1H}^\dagger + \hat{b}_{2V}^\dagger) (\hat{b}_{1H}^\dagger - \hat{b}_{2V}^\dagger) |vac\rangle \quad (D2)$$

- Step 3

$$\frac{1}{4} (\hat{a}_{1D}^\dagger + \hat{b}_{2A}^\dagger) (\hat{a}_{1D}^\dagger - \hat{b}_{2A}^\dagger) (\hat{b}_{1D}^\dagger + \hat{a}_{2A}^\dagger) (\hat{b}_{1D}^\dagger - \hat{a}_{2A}^\dagger) |vac\rangle \quad (D3)$$



- Step 4

$$\begin{aligned}
& \frac{1}{16} \left( (\hat{a}_{1H}^\dagger + \hat{a}_{2V}^\dagger) + (\hat{b}_{2H}^\dagger - \hat{b}_{1V}^\dagger) \right) \left( (\hat{a}_{1H}^\dagger + \hat{a}_{2V}^\dagger) - (\hat{b}_{2H}^\dagger - \hat{b}_{1V}^\dagger) \right) \\
& \times \left( (\hat{b}_{1H}^\dagger + \hat{b}_{2V}^\dagger) + (\hat{a}_{2H}^\dagger - \hat{a}_{1V}^\dagger) \right) \left( (\hat{b}_{1H}^\dagger + \hat{b}_{2V}^\dagger) - (\hat{a}_{2H}^\dagger - \hat{a}_{1V}^\dagger) \right) |vac\rangle \\
& = \frac{1}{16} \left( \hat{a}_{1H}^{\dagger 2} + 2\hat{a}_{1H}^\dagger \hat{a}_{2V}^\dagger + \hat{a}_{2V}^{\dagger 2} - \hat{b}_{2H}^{\dagger 2} + 2\hat{b}_{2H}^\dagger \hat{b}_{1V}^\dagger - \hat{b}_{1V}^{\dagger 2} \right) |vac\rangle \\
& \quad \times \left( \hat{b}_{1H}^{\dagger 2} + 2\hat{b}_{1H}^\dagger \hat{b}_{2V}^\dagger + \hat{b}_{2V}^{\dagger 2} - \hat{a}_{2H}^{\dagger 2} + 2\hat{a}_{2H}^\dagger \hat{a}_{1V}^\dagger - \hat{a}_{1V}^{\dagger 2} \right) |vac\rangle, \tag{D4}
\end{aligned}$$

- Step 5

$$\frac{1}{4} \left( (\hat{a}_{1H}^\dagger \hat{b}_{1H}^\dagger + \hat{a}_{1V}^\dagger \hat{b}_{1V}^\dagger) (\hat{a}_{2H}^\dagger \hat{b}_{2H}^\dagger + \hat{a}_{2V}^\dagger \hat{b}_{2V}^\dagger) + (\hat{a}_{1H}^\dagger \hat{b}_{1V}^\dagger + \hat{a}_{1V}^\dagger \hat{b}_{1H}^\dagger) (\hat{a}_{2H}^\dagger \hat{b}_{2H}^\dagger - \hat{a}_{2V}^\dagger \hat{b}_{2V}^\dagger) \right) |vac\rangle \tag{D5}$$

At Step 5, we sort out the states that click one of the two detectors in each PBS. When the two heralding detectors receive photons of the same polarization, we obtain a Bell state  $\frac{1}{\sqrt{2}}(|HH\rangle + |VV\rangle)$ . When the two heralding detectors receive photons of the opposite polarization, we obtain a different Bell state  $\frac{1}{\sqrt{2}}(|HH\rangle - |VV\rangle)$ .

- 
- |  |   |
|--|---|
| <p>[1] Ryszard Horodecki, Paweł Horodecki, Michał Horodecki, and Karol Horodecki. Quantum entanglement. <i>Reviews of Modern Physics</i>, 81(2):865, 2009.</p> <p>[2] Nicolas Gisin, Grégoire Ribordy, Wolfgang Tittel, and Hugo Zbinden. Quantum cryptography. <i>Reviews of modern physics</i>, 74(1):145, 2002.</p> <p>[3] Stefano Pirandola, Ulrik L Andersen, Leonardo Banchi, Mario Berta, Darius Bunandar, Roger Colbeck, Dirk Englund, Tobias Gehring, Cosmo Lupo, Carlo Ottaviani, et al. Advances in quantum cryptography. <i>Advances in optics and photonics</i>, 12(4):1012–1236, 2020.</p> <p>[4] Emanuel Knill, Raymond Laflamme, and Gerald J Milburn. A scheme for efficient quantum computation with linear optics. <i>nature</i>, 409(6816):46–52, 2001.</p> <p>[5] John Preskill. Quantum computing in the nisq era and beyond. <i>Quantum</i>, 2:79, 2018.</p> <p>[6] Paul Adrien Maurice Dirac. <i>The principles of quantum mechanics</i>. 27. Oxford university press, 1981.</p> <p>[7] Malte C Tichy, Fernando de Melo, Marek Kuś, Florian Mintert, and Andreas Buchleitner. Entanglement of identical particles and the detection process. <i>Fortschritte der Physik</i>, 61(2-3):225–237, 2013.</p> <p>[8] Mario Krenn, Armin Hochrainer, Mayukh Lahiri, and Anton Zeilinger. Entanglement by path identity. <i>Physical Review Letters</i>, 118(8):080401, 2017.</p> <p>[9] Rosario Lo Franco and Giuseppe Compagno. Indistinguishability of elementary systems as a resource for quantum information processing. <i>Physical Review Letters</i>, 120(24):240403, 2018.</p> <p>[10] Seungbeom Chin and Joonsuk Huh. Entanglement of identical particles and coherence in the first quantization language. <i>Physical Review A</i>, 99(5):052345, 2019.</p> | <p>[11] Farzam Nosrati, Alessia Castellini, Giuseppe Compagno, and Rosario Lo Franco. Robust entanglement preparation against noise by controlling spatial indistinguishability. <i>npj Quantum Information</i>, 6(1):1–7, 2020.</p> <p>[12] Mariana R Barros, Seungbeom Chin, Tanumoy Pramanik, Hyang-Tag Lim, Young-Wook Cho, Joonsuk Huh, and Yong-Su Kim. Entangling bosons through particle indistinguishability and spatial overlap. <i>Optics Express</i>, 28(25):38083–38092, 2020.</p> <p>[13] Bernard Yurke and David Stoler. Einstein-podolsky-rosen effects from independent particle sources. <i>Physical Review Letters</i>, 68(9):1251, 1992.</p> <p>[14] Bernard Yurke and David Stoler. Bell’s-inequality experiments using independent-particle sources. <i>Physical Review A</i>, 46(5):2229, 1992.</p> <p>[15] Paweł Blasiak and Marcin Markiewicz. Entangling three qubits without ever touching. <i>Scientific Reports</i>, 9, 2019.</p> <p>[16] Bruno Bellomo, Rosario Lo Franco, and Giuseppe Compagno. N identical particles and one particle to entangle them all. <i>Physical Review A</i>, 96(2):022319, 2017.</p> <p>[17] Yong-Su Kim, Young-Wook Cho, Hyang-Tag Lim, and Sang-Wook Han. Efficient linear optical generation of a multipartite W state via a quantum eraser. <i>Physical Review A</i>, 101(2):022337, 2020.</p> <p>[18] Mario Krenn, Xuemei Gu, and Anton Zeilinger. Quantum experiments and graphs: Multipartite states as coherent superpositions of perfect matchings. <i>Physical Review Letters</i>, 119(24):240403, 2017.</p> <p>[19] Xuemei Gu, Manuel Erhard, Anton Zeilinger, and Mario Krenn. Quantum experiments and graphs II: Quantum interference, computation, and state generation. <i>Proceedings of the National Academy of Sciences</i>, 116(10):4147–4155, 2019.</p> |
|--|---|

- [20] Xuemei Gu, Lijun Chen, Anton Zeilinger, and Mario Krenn. Quantum experiments and graphs. III. high-dimensional and multiparticle entanglement. *Physical Review A*, 99(3):032338, 2019.
- [21] Pawel Blasiak, Ewa Borsuk, Marcin Markiewicz, and Yong-Su Kim. Efficient linear-optical generation of a multipartite W state. *Physical Review A*, 104(2):023701, 2021.
- [22] Seungbeom Chin, Yong-Su Kim, and Sangmin Lee. Graph picture of linear quantum networks and entanglement. *Quantum*, 5:611, 2021.
- [23] Manuel Erhard, Mehul Malik, Mario Krenn, and Anton Zeilinger. Experimental greenberger–horne–zeilinger entanglement beyond qubits. *Nature Photonics*, 12(12):759–764, 2018.
- [24] Donghwa Lee, Tanumoy Pramanik, Seongjin Hong, Young-Wook Cho, Hyang-Tag Lim, Seungbeom Chin, and Yong-Su Kim. Entangling three identical particles via spatial overlap. *Optics Express*, 30(17):30525–30535, 2022.
- [25] Mercedes Gimeno-Segovia, Pete Shadbolt, Dan E Browne, and Terry Rudolph. From three-photon greenberger–horne–zeilinger states to ballistic universal quantum computation. *Physical review letters*, 115(2):020502, 2015.
- [26] Mihir Pant, Don Towsley, Dirk Englund, and Saikat Guha. Percolation thresholds for photonic quantum computing. *Nature communications*, 10(1):1–11, 2019.
- [27] Madelyn Glymour, Judea Pearl, and Nicholas P Jewell. *Causal inference in statistics: A primer*. John Wiley & Sons, 2016.
- [28] Valentin Gebhart, Luca Pezzè, and Augusto Smerzi. Genuine multipartite nonlocality with causal-diagram postselection. *Physical Review Letters*, 127(14):140401, 2021.
- [29] Stefanie Barz, Gunther Cronenberg, Anton Zeilinger, and Philip Walther. Heralded generation of entangled photon pairs. *Nature Photonics*, 4(8):553–556, 2010.
- [30] Claudia Wagenknecht, Che-Ming Li, Andreas Reingruber, Xiao-Hui Bao, Alexander Goebel, Yu-Ao Chen, Qiang Zhang, Kai Chen, and Jian-Wei Pan. Experimental demonstration of a heralded entanglement source. *Nature Photonics*, 4(8):549–552, 2010.
- [31] Heonoh Kim, Hee Su Park, and Sang-Kyung Choi. Three-photon N00N states generated by photon subtraction from double photon pairs. *Optics Express*, 17(22):19720–19726, 2009.
- [32] Young-Sik Ra, Hyang-Tag Lim, Joo-Eon Oh, and Yoon-Ho Kim. Phase and amplitude controlled heralding of N00N states. *Optics Express*, 23(24):30807–30814, 2015.
- [33] Scott B Papp, Kyung Soo Choi, Hui Deng, Pavel Lougovski, SJ Van Enk, and HJ Kimble. Characterization of multipartite entanglement for one photon shared among four optical modes. *Science*, 324(5928):764–768, 2009.
- [34] Ido Schwartz, Dan Cogan, Emma R Schmidgall, Yaroslav Don, Liron Gantz, Oded Kenneth, Neta H Lindner, and David Gershoni. Deterministic generation of a cluster state of entangled photons. *Science*, 354(6311):434–437, 2016.
- [35] J Shi, P Xu, ML Zhong, YX Gong, YF Bai, WJ Yu, QW Li, H Jin, and SN Zhu. Heralded generation of multipartite entanglement for one photon by using a single two-dimensional nonlinear photonic crystal. *Optics Express*, 21(7):7875–7881, 2013.
- [36] Armin Tavakoli, Géraldine Haack, Nicolas Brunner, and Jonatan Bohr Brask. Autonomous multipartite entanglement engines. *Physical Review A*, 101(1):012315, 2020.
- [37] FV Gubarev, IV Dyakonov, M Yu Saygin, GI Struchalin, SS Straupe, and SP Kulik. Improved heralded schemes to generate entangled states from single photons. *Physical Review A*, 102(1):012604, 2020.
- [38] Dat Thanh Le, Warit Asavanant, and Nguyen Ba An. Heralded preparation of polarization entanglement via quantum scissors. *Physical Review A*, 104(1):012612, 2021.
- [39] Marcin Karczewski, Su-Yong Lee, Junghee Ryu, Zakarya Lasmar, Dagomir Kaszlikowski, and Pawel Kurzyński. Sculpting out quantum correlations with bosonic subtraction. *Physical Review A*, 100(3):033828, 2019.
- [40] MS Kim, H Jeong, A Zavatta, V Parigi, and M Bellini. Scheme for proving the bosonic commutation relation using single-photon interference. *Physical Review Letters*, 101(26):260401, 2008.
- [41] A Zavatta, V Parigi, MS Kim, H Jeong, and M Bellini. Experimental demonstration of the bosonic commutation relation via superpositions of quantum operations on thermal light fields. *Physical Review Letters*, 103(14):140406, 2009.
- [42] Valentina Parigi, Alessandro Zavatta, Myungshik Kim, and Marco Bellini. Probing quantum commutation rules by addition and subtraction of single photons to/from a light field. *Science*, 317(5846):1890–1893, 2007.
- [43] Alexei Ourjoumtsev, Rosa Tualle-Brouiri, Julien Laurat, and Philippe Grangier. Generating optical schrodinger kittens for quantum information processing. *Science*, 312(5770):83–86, 2006.
- [44] Lin Htoo Zaw, Zakarya Lasmar, Chi-Huan Nguyen, Ko-Wei Tseng, Dzmitry Matsukevich, Dagomir Kaszlikowski, and Valerio Scarani. Sculpting bosonic states with arithmetic subtractions. *New Journal of Physics*, 24(8):083023, 2022.
- [45] José Ignacio Latorre and MA Martín-Delgado. Majorization arrow in quantum-algorithm design. *Physical Review A*, 66(2):022305, 2002.
- [46] Roman Orus, José I Latorre, and Miguel A Martín-Delgado. Systematic analysis of majorization in quantum algorithms. *The European Physical Journal D-Atomic, Molecular, Optical and Plasma Physics*, 29(1):119–132, 2004.
- [47] Seungbeom Chin and Joonsuk Huh. Majorization and the time complexity of linear optical networks. *Journal of Physics A: Mathematical and Theoretical*, 52(24):245301, 2019.
- [48] Carlos Ruiz-Gonzalez, Sören Arlt, Jan Petermann,

- Sharareh Sayyad, Tareq Jaouni, Ebrahim Karimi, Nora Tischler, Xuemei Gu, and Mario Krenn. Digital discovery of 100 diverse quantum experiments with pytheus. *arXiv preprint arXiv:2210.09980*, 2022.
- [49] Mark Um, Junhua Zhang, Dingshun Lv, Yao Lu, Shuoming An, Jing-Ning Zhang, Hyunchul Nha, MS Kim, and Kihwan Kim. Phonon arithmetic in a trapped ion system. *Nature Communications*, 7(1):1–7, 2016.
- [50] Mario Krenn, Mehul Malik, Manuel Erhard, and Anton Zeilinger. Orbital angular momentum of photons and the entanglement of laguerre–gaussian modes. *Philosophical Transactions of the Royal Society A: Mathematical, Physical and Engineering Sciences*, 375(2087):20150442, 2017.
- [51] Marc Hein, Wolfgang Dür, Jens Eisert, Robert Raussendorf, M Nest, and H-J Briegel. Entanglement in graph states and its applications. *arXiv preprint quant-ph/0602096*, 2006.
- [52] Adán Cabello. N-particle N-level singlet states: some properties and applications. *Physical Review Letters*, 89(10):100402, 2002.
- [53] Marcin Karczewski, Robert Pisarczyk, and Paweł Kurzyński. Genuine multipartite indistinguishability and its detection via the generalized hong-ou-mandel effect. *Physical Review A*, 99(4), April 2019.
- [54] Michael Walter, David Gross, and Jens Eisert. Multipartite entanglement. *Quantum Information: From Foundations to Quantum Technology Applications*, pages 293–330, 2016.
- [55] Seungbeom Chin. Coherence number as a discrete quantum resource. *Physical Review A*, 96(4):042336, 2017.